Ultrastructural Deformations and Proprioceptive Function in Human Teeth

Jay Harris Levy, DDS, BSME*†

Private practice, New York, N.Y.

*Former Clinical Assistant Professor of Comprehensive Care & Applied Practice Administration and Behaviorial Sciences. New York University College of Dentistry, New York, NY.

†Address correspondence to:

Dr. Jay Harris Levy
140 East 52nd Street, Suite 2C
New York, NY 10022
U.S.A.

Telephone:

(212) 751-4630 - office
(212) 751-4634 - fax
(203) 333-1501 - home

ABSTRACT

A theory of intradental proprioception is presented which proposes that strains in dentin arising from occlusal forces induce dentinal fluid flow which initiates nerve action potential generation along sensory nerve fibers in odontoblastic tubules. A structural analysis based on the theory of mechanics of materials is utilized to predict stress patterns in teeth under load. The results reveal the oral musculature is capable of generating biting forces and intradental stresses significantly greater than the strengths of tooth materials. Lateral force components of occlusal tooth contacts can generate extreme stress elevations in the cervical regions of teeth due to the introduction of bending stresses. The results compare favorably to other structural investigations and to neurophysiologic studies which have found that strains in dentin produce reflex responses in the oral musculature. It is postulated that abfraction lesions are fatigue failures in the cervical region of teeth. Abfractions progress slowly through teeth due to intradental proprioceptive reflex regulatory control of the oral musculature. It is proposed that teeth be considered specialized tactile-musculoskeletal organs of mastication. Applications of these hypotheses are extensive. They include both prevention and treatment elements and they support the clinical analysis and proper equilibration of occlusions.

INTRODUCTION

Teeth are complex structural members which possess elaborate integral neural sensory networks. The purpose of this article is to investigate the ultrastructural and neurophysiologic effects of occlusal forces on teeth. The method utilized is a structural analysis based on the theory of mechanics of materials. This method allows for the simplified visualization of stress patterns which are created under varied load conditions. The behavior of teeth under load will be evaluated and correlated with neurophysiologic, ultrastructural, biomechanical and clinical findings.

The application of forces to a solid body creates a state of stress within the body; the physical response of the body is deformation or fracture. Mechanics of materials investigates "the nature of forces set up within a body to balance externally applied forces" (Popov, 1976). This analytic method uses simplifications and assumptions to model the behavior of a body subjected to load. All simplifications and assumptions applied must be evaluated and correlated with clinical observations before conclusions may be drawn.

The method of sections is utilized to investigate the state of stress at a section within a body. Examination of an infinite number of small particles within a section creates an analog view of the stress states within the section. Free body diagram sketches of the body are used to visualize all forces acting on it. Materials are assumed to be isotropic, homogeneous and elastic. Teeth are orthotropic-heterogeneous bodies which, when loaded, respond with a highly varied internal stress distribution. They exhibit both elastic and viscoelastic properties. The computational results obtained utilizing the theory of mechanics of materials are statistical average values which are highly significant quantities provided reasonable simplifications and assumptions have been applied (Popov, 1976).

Various researchers have modeled teeth utilizing the finite element analysis technique (FEA). They have made observations and drawn conclusions based on their simplifications and assumptions. Plane strain FEA and axisymmetric FEA are sophisticated investigative tools which have limitations. Geometry is altered, boundary conditions are difficult to model and specific material properties of complex intradental materials are assumed based on the highly varied available data. This variability of data reflects small test material sample size and the high degree of orthotropic-heterogeneity characteristic to tooth materials (Kawamura, 1976). The computational results achieved by FEA are also statistically valid provided all simplifications and assumptions are carefully considered.

Abfractions are commonly observed saucer shaped and "V" shaped notches in cervical dentin. It has been proposed by Lee and Eakle (1984) and Grippo (1991) that abfractions originate in the fracture of elements of highly stressed cervical dentin. This article will investigate the etiology of abfractions and discuss the behavior of teeth severely weakened by abfractions.

Neurophysiologic research has demonstrated several important masticatory neuromuscular reflexes. They include jaw opening, jaw closing, lateral jaw and jar reflexes. These reflexes are critical to the coordination of mastication. The principle proprioceptors of chewing reflexes have been theorized to exist within the periodontal tissues. Definitive periodontal mechano-proprioceptors have not been identified in sufficient numbers to account for the exquisite sensitivity the proprioceptive-neuromusculature exhibits during mastication (Lavelle, 1988; Taylor, 1990). The abundance of intradental sensory enervation is a well established fact. The functional significance of this phenomenon has never been adequately explained. The major function given to this enervation has been pain perception. This article presents evidence that the functional-anatomic basis for the abundant sensory enervation of teeth is proprioception during mastication.

MATERIALS AND METHODS

Ultrastructure

Teeth are composite structures consisting of enamel, dentin, pulp and cementum. Each of these component materials has unique directional mechanical properties. Currently accepted average values of some of the material properties of dentin and enamel appear in Table 1 (O'Brien, 1989).

Enamel is the hardest material in the human body. It may be classified as a brittle material due to the large value of its elastic modulus, low tensile strength and the proximity of its proportional limit and ultimate compressive strength on a stress strain curve (Phillips, 1973). Enamel is composed of 95% inorganic crystalline hydroxyapatite, 4% water and 1% organic material. Hydroxyapatite crystals are arranged in rods which originate at the dento-enamel junction (DEJ) and follow straight or gently curved paths to the enamel surface. The DEJ is the region where dentin and enamel fuse. Arsenault and Robinson (1989) have demonstrated the intimate relationship that enamel rods and dentin apatite crystals possess as they oppose each other at the DEJ. They have also demonstrated fraying and marked widening of the highly calcified terminal ends of mantle dentin collagen fibers as they interweave with the bases of enamel rod structures in this region. Their microanalytical study has suggested that the DEJ is a transition zone where enamel crystals arise and grow from existing dentin crystals. The underlying mantle dentin zone is the first dentin layer formed. It has larger collagen fibers (100 to 200 nm in diameter), fewer defects, and it is slightly less mineralized than the main body of dentin. Globular dentin separates mantle dentin and dentin . This zone has been interpreted as an area of imperfect calcification of dentin (Avery, 1992).

Dentin is more elastic than enamel. Its composition is 70% inorganic material, 20% organic material and 10% water. It has an ultrastructure which is most readily identified by the odontoblastic tubule (OT), (Fig. 1 and Fig. 2). As a structural material it exhibits anisotropic properties. It is stiffer when loaded parallel to the OTs and more flexible in a perpendicular

direction (Caputo and Standlee, 1987). The directional elasticity of dentin serves to minimize shear stress at the DEJ and prevents fracture of the brittle enamel cap. Odontoblastic tubules are composed of odontoblastic processes of pulpal odontoblasts, pulpal nerve fibers and peri-odontoblastic fluid, surrounded by hard highly calcified layer of peritubular dentin. Peritubular dentin walls contain an abundance of tightly packed, concentrically wound collagen fibers and are periodically fenestrated by canaliculi. OTs course from the pulp through dentin, globular dentin, mantle dentin and terminate at the DEJ. The lumens of OTs may calcify in the process of forming sclerotic dentin. Intertubular dentin surrounds peritubular dentin and is composed of an organic matrix of collagen fibers (50 to 200 nm in diameter) and inorganic hydroxyapatite crystals. It is less calcified than peritubular dentin and its fibers are generally oriented perpendicular to the OTs. These inter-odontoblastic fibers form a meshwork which connects OTs (Sogaard-Pedersen *et al.*, 1990). OTs have a density of 30,000 to 60,000 per square millimeter near the pulp (Garberoglio and Brannstrom, 1976; Fosse *et al.*, 1992). OT density decreases volumetrically as the dento-enamel junction (DEJ) is approached. This occurs with a concurrent increase in intertubular collagen fiber span and a narrowing of OTs (Avery 1992). Predentin is a transition tissue between dentin and pulp tissues. It has a collagen ultrastructure which is less mineralized than that of dentin. In their scanning electron microscope (SEM) micrographs Marion *et al.* (1991) have brilliantly captured the porous, sponge-like appearance of predentin.

Several researchers have elaborated on the contents of the OT. Szabó, Trombitás and Szabó (1984) described the cable-like appearance of the odontoblastic process (OP) as it courses through the OT. They also described thin fibers accompanying the OP which they hypothesized to be nerve fibers. Frank (1968) described complex infoldings of nerve fibers within concavities of OPs. He observed attachment sites between OPs and nerve fibers which appeared to be tight junctions. Holland (1976) observed gap junctions between nerve fibers and odontoblasts. Byers and Kish (1976) using radioautographic tracing have demonstrated nerve fibers which spiral around OPs as they course through predentin and dentin. Arwill *et al.* (1973) have verified that these fibers are sensory in nature, and they named odontoblast-nerve fibers "intradental sensory units".

The ultrastructure of the tooth pulp consists of a loose collagen web which suspends odontoblasts, nervous tissues, vascular tissue and fibroblasts. The odontoblastic zone occupies the region immediately below circumpulpal dentin and is further divided into a layer of odontoblasts, a cell free zone and a cell rich zone. The parietal layer of nerves lines the internal aspect of the odontoblastic zone. Deeper layers of pulpal tissues consist of aggregates of these tissue components, with blood vessels and nerve fibers increasing in size centrally and apically.

Tooth model

The model utilized in this investigation is of a left maxillary central incisor illustrated in

Fig. 3. It was selected for its relatively simple geometric form. Dental anatomy and dimensions were adapted and simplified from "Dental Anatomy and Occlusion" by Kraus *et al.* (1969). A tooth can be considered a cantilevered beam of varied cross-sectional area. More specifically a tooth is a cantilevered (free standing) beam-post subject to axial and lateral forces and fixed at its end. The instantaneous support of a tooth can be simplified as a fixed support. The method of sections will be applied to the model and free body diagram representations of the clinical crown will be analyzed. Because an established mechanical principle is that bending moments are greatest at the support of a cantilevered beam sections will be analyzed in the region of bone support just above the crest of bone in two situations: 0% bone loss and 30% bone loss (Popov, 1976). 25 lb (111 N) forces will be applied first axially then inclined at 45 degrees. This force magnitude was chosen as an intermediate value of functional occlusal force. The maximum published values of occlusal forces observed clinically on incisors varies in the literature and ranges between 45 lb (200 N) and 55 lb (245 N) (Caputo and Standlee, 1987; Phillips, 1973).

All elements within the tooth are subject to normal, shear and torsional stresses. The elements which are to be analyzed are subjected to compound stress and will be evaluated by applying the fundamental formulas of mechanics presented in Fig. 4 (Popov, 1976). Computational procedures appear in the appendix.

Axial loading

A 25 lb (111 N) axial occlusal force is applied to the maxillary central incisor model. It is assumed that the force acts through the neutral axis of the tooth and that the tooth is isotropic, homogeneous and elastic. Lateral forces are absent. Two sections of the tooth will be studied: Section A is located approximately at the crest of bone in dentin and Section B represents a 30% loss of supporting bone (Fig. 5). It is assumed that these sections are round with round pulpal cavities. A maxillary central incisor has been selected as the model because of the approximate accuracy of this assumption. This simple loading condition eliminates direct bending, shear and torsional stresses from sections A and B. These sections are subject to normal axial stress. Fig. 5 contains free body diagrams representing the normal stress at the two sections. Results are listed in Table 2.

Inclined loading

A 25 lb (111 N) force is applied at a 45 degree angle to the lingual surface of the tooth model 0.078 in. (2.0 mm) below the incisal edge and 0.039 in. (1.0 mm) lingual to the neutral axis. The force vector intersects the neutral axis. The same material assumptions, tooth geometry and sections as in the axial loading analysis apply. Only loading geometry is varied. Fig. 6 shows free body diagrams representing normal stress at sections A and B. Table 3 lists the results.

Laws of transformation allow for the rotation of stressed material elements providing equivalent elemental stresses. The orientation of planes of maximum shear and maximum normal

stresses can be determined in this manner. Dentin is weak in shear as indicated in Table 1. Thus, a material element in dentin which is subject to primarily compressive or tensile stress contains planes of shear stress which attempt to slide past each other. In this example the state of stress of element B_1 is a compressive stress of 12,880 lb/in^2 (88.8 MPa) and 0 lb/in^2 shear stress. Utilizing the Mohr's circle of stress analytical technique the equivalent maximum shear stress acting on this element may be calculated (Popov, 1976). The maximum shear stress acting on element B_1 occurs when the element is rotated 45 degrees. The equivalent stresses with the element oriented in this manner are compressive normal stresses of 6,440 lb/in^2 (44.4 MPa) acting on all sides of the element and 6,440 lb/in^2 (44.4 MPa) positive shear (Fig 7).

Hooke's law (Eq-5) states that stress (σ) is proportional to strain (ϵ), with the modulus of elasticity (E) being the constant of proportionality: $\sigma = E\epsilon$. Strain is defined as deformation (Δ) per unit length (L): $\epsilon = \Delta / L$. The assumptions applied in its usage are that materials are elastic and that the proportional limits of materials are not exceeded. Fosse, Saele and Eide (1992) discussed the concept of secretory odontoblastic territory (SOT). The SOT is the sum of dentin material produced by one odontoblast. According to their data, an acceptable approximation of mean surface density of odontoblastic tubules at element B_1 would be 18,000/mm^2 and the density at element B_2 would be 50,000/mm^2. One SOT extending from B_1 to B_2 can be modeled as a long tapering square solid with the OT in the center (Fig. 8). The thickness of this tapered square solid varies from 7.46×10^{-3} mm at the surface of the tooth to 4.47×10^{-3} mm at the pulp. The taper of the SOT is therefore 1.67 :1. The calculated normal compressive stress levels at elements B_1 and B_2 are 12,880 lb/in^2 (88.9 MPa) and 3,540 lb/in^2 (24.4 MPa) respectively. Assuming the modulus of elasticity of dentin to be $2.65(10^6)$ lb/in^2 (18.3 GPa) we can calculate the strains at elements B_1 and B_2 to be 0.00486 and 0.00134 respectively. These strain levels are below the maximum strain levels for permanent deformation of dentin which, according to Braden (1976) are 0.010-0.015. By multiplying the strains at B_1 and B_2 by the SOT thicknesses the deformation of the solid may be calculated (B_1=$3.63(10^{-5})$mm, B_2=$5.99(10^{-6})$mm). The ratio of deformation of this SOT is 6.05:1 comparing the surface to pulpal ends. A significant shear stress gradient also exists along the length of this SOT; 0 lb/in^2 (0 MPa) at B_1 increasing to 810 lb/in^2 (5.6 MPa) at B_2.

Lateral loading with 50% abfraction

In analyzing the 50% abfraction illustrated in Fig. 9 the following assumptions are made. This abfraction has reduced by 50% the cross-sectional area of the maxillary central incisor illustrated in Fig 3 with 30% bone loss (section B). The reduced section is a semicircular area (secondary dentin replaces the pulp chamber), $I = 8.59(10^{-6})$in.^{4} (3.6 mm^4) and c = 0.054 in. (1.4 mm). The allowable UTS of dentin is 6000 lb/in.^{2} (41.4 MPa) and a lateral force is applied 0.078 in. (2.0 mm) below the incisal edge. Utilizing equation (2) and $M=F_X(L')$, it is calculated that a lateral force of 1.95 lb (8.7 N) induces cervical tensile stress in element B_5 equal to the

assumed UTS of dentin. 1.95 lb (8.7 N) is the maximum lateral load carrying capacity of this weakened tooth.

Fatigue strength estimate

Dentin has an average published ultimate tensile strength (UTS) of 6,750 lb/in^2 (46.6 MPa) based on static testing (O'Brien, 1989). Teeth are subject to cyclic loading conditions, and it has been established that materials subjected to cyclic loading conditions fail at stress levels which are significantly lower than under static loading. Currently there are no published values for endurance limits (k_e) for tooth materials. For cyclic loading conditions the allowable stress for steel would be 60% of static allowable stress (k_e=0.6). This factor is intended to take into account material non-uniformity, internal material deformations, variations in loading intensity and the additive effects of cyclic loading conditions. Utilizing this design factor for dentin in tension an estimated maximum working strength of dentin ($S_{working}$) is:

$S_{working}= k_e S_{UTS}=(0.6)(6750\ lb/in^2)= 4{,}050\ lb/in.^2$ (27.9 MPa).

RESULTS

The axial loading analysis predicts uniform low stress values obtained under this loading condition (Table 2). The inclined loading analysis introduces a lateral force component into the loading geometry of the model tooth and the results indicate that extreme stress elevations develop in the buccal and lingual cervical regions of teeth due to the generation of bending moments (Table 3). Increases in crown to root ratios as a result of periodontal disease result in longer moment arms and increased bending stresses. A factor of greater significance is the reduction of cross-sectional area and area moment of inertia due to loss of supporting bone and conical root form. The area moment of inertia of a beam can be the most significant factor determining the load carrying capacity of the beam. Cantilevered beams with thin cross-sections at their highly stressed supports are inherently weak. The lateral loading with 50% abfraction analysis calculated that a 1.95 lb. (8.7 N) force would cause a tensile failure in the weakened model tooth. The intact section with a pulp space would fail in tension when subjected to a 8.00 lb (35.6 N) lateral force. This illustrates that severe abfractions significantly reduce the area moment inertia of a tooth and significantly reduce the load carrying capacity of that tooth. A 50% reduction in cross sectional area results in a 75% reduction in strength.

Comparing the extreme stress levels achieved in the root sections of the inclined loading analysis to tooth material properties reveals that the resultant normal stress at element B_5 (+11,520 lb/in^2 (+79.5 MPa)) exceeds the maximum published ultimate tensile strength (UTS) of dentin (7,500 lb/in.^{2} (51.7 MPa)) by a significant margin. This observation leads to the conclusion that the load carrying capacity of the tooth has been exceeded and that immediate failure will occur. The facts that published, experimentally derived, maximum bite force values for human incisors exceed 45 lb (200 N), and that a force of 25 lb (111 N) applied to the model incisor results in

failure, indicate the need to reevaluate the methods which have been utilized to obtain maximum bite force values.

The maximum tensile stress achieved in element A_5 in the inclined loading analysis is 4,080 lb/in^2 (28.1MPa). This value exceeds the estimated working strength of dentin for cyclic loading conditions ($S_{working}$=4,050 lb/in.^{2} (27.9 MPa)). Therefore, given a high number of cyclic loads of 25 lbs (111N) directed at a 45 degree angle, it may be expected that element A_5 will undergo fatigue failure. In clinical situations over a long period of time, maxillary central incisors may be subject to cyclic forces of 50 lbs (222 N) under similar geometric conditions. This force generates a maximum tensile stress of 8,160 lb/in.^{2}(56.3MPa) in element A_5 which would clearly cause immediate failure. Eccentric tooth contacts can induce additional torsional shear stresses (τ_T) in elements where the state of stress due to axial normal stress (σ_A), bending normal stress (σ_B) and lateral force induced shear stress (τ_L) and is already critically close to failure.

The stress gradient between elements B_1 and B_2 in the inclined loading analysis causes differential compression of the SOT illustrated in Fig. 8 in accordance with Hooke's Law. Most material deformation should occur in intertubular dentin due to its reduced calcification and stiffness as compared to peritubular dentin. Regions of dentin under tension will undergo stretching of intertubular collagen fibers and regions under compression will undergo compaction of collagen fibers. SOT geometry exaggerates the effects of differential stress and stiffness. These differential stresses compress intertubular dentin and bend the peripheral ends of OTs apically. Assuming dentinal fluid acts as an incompressible fluid then the deformations in a SOT will induce a volume of fluid flow equal to the volume of the deformation of the SOT. The rigid ultrastructure of the OT serves as a conduit for dentinal fluid to flow toward the pulp (from a region of high pressure to a region of low pressure).

DISCUSSION

The structural analyses finds that lateral occlusal forces generate bending moments which cause extreme normal stress elevations in cervical elements of dentin. Normal stress in dentin decreases linearly as the neutral axis of the tooth model is approached. The numerical results obtained must be considered approximations of stress levels achieved during mastication due to the simplifications and assumptions made. Yettram, Wright and Pickard (1976) analyzed a two dimensional finite element model of a mandibular second premolar loaded with an occlusal force inclined toward the buccal and demonstrated significant stress elevations in buccal cervical dentin. Their findings revealed a differential stress gradient between superficial, buccal cervical dentin and pulpal, cervical dentin similar to the present results. Thresher and Saito (1973) also demonstrated buccal and lingual bending moment induced cervical stress elevations in their plane strain finite element analysis models of maxillary central incisors. In their studies they considered both homogeneous and non-homogenous tooth models. They showed significant coronal tooth bending

as a result of lateral force induced displacement of the enamel cap. Darendeliler, Darendeliler and Kinoglu (1992) in their three dimensional finite element model of a maxillary central incisor showed trends of elevated cervical stress as a result of bending moments and high stress values at the apical terminus of the DEJ. Other authors utilizing FEA have observed similar trends (Farah *et al.*, 1973; Hoijatie and Anusavice, 1990; Selna *et al.*, 1975; Goel *et al.*, 1990).

Abundant neurophysiologic research has been done which correlates force application to teeth with neuromuscular responses. Bjorland *et al.* (1991) have shown that tooth taps evoke the jaw opening reflex. Gurza, Lowe and Sessle (1976) have demonstrated that this reflex produces a silent period in masseter muscle activity. The length of this silent period is proportional to the intensity of the tooth tap. They also noted that a graded inhibitory effect occurred in this reflex. Stimulation of a tooth pulp produced greater suppression of masseteric activity than a tooth tap.

Numerous studies have been published which correlate jaw reflexes and periodontal mechanoreceptors (Taylor, 1990). There is undoubtedly a significant periodontal proprioceptive component in mastication. The relative importance of intrapulpal, periodontal, osseous, muscular and joint proprioception requires additional research using improved techniques to isolate individual components of the masticatory system. According to Matthews (1981), "We have become increasingly aware that the properties of the receptor system in teeth may be influenced by the experimental techniques we employ to record from nerves.". Minimally invasive studies and others utilizing improved isolating techniques have demonstrated intradental proprioception. Olgart, Gazelius and Sundstrom (1988) demonstrated that isolated bending stress applied to cat canine teeth excites fast conducting intradental A-fibers which induce the jaw opening reflex. They also demonstrated that removal of coronal tooth pulp abolishes this reflex. They concluded that a specialized sensory transducer mechanism exists in dentin and that it is activated by deformation of the clinical crown of a tooth. McGrath *et al.* (1981) demonstrated in human subjects utilizing electrical stimulation that the threshold of initial detection by tooth pulp afferents is well below the threshold of pain. They also showed that the silent period in masseter muscle activity is first elicited at the threshold of initial detection.

Dong, Erich, Chudler and Martin (1985) discovered that intradental receptors generated neural spike discharges in myelinated A-δ and A-β nerve fibers in response to mechanical transient forces applied to canine teeth of cats. They clearly demonstrated that these neural discharges exhibit unique discharge signatures or frequency codes depending on the surface roughness of objects rubbed against the enamel surface of a vital tooth. These discharges, which were generated by low threshold, non-nociceptive stimulation of intradental proprioceptors, were recorded in the trigeminal semilunar ganglion. Dong *et al.* (1993) demonstrated differences in dynamic response characteristics between periodontal mechanoreceptors (PDLMs) and intradental mechanoreceptors (IMs) in canine teeth of cats. IMs responded to higher frequency mechanical tooth stimulation than

PDLMs. PDLMs demonstrated lower mechanical stimulus thresholds than IMs. They concluded that "Periodontal mechanoreceptors and intradental mechanoreceptors appear to provide a continuum of dynamic afferent inputs necessary for tactile sensibility of teeth.". These findings support the hypothesis that tooth pulp afferents function primarily as proprioceptors and secondarily as nociceptors.

It has been widely observed that non-vital teeth fracture in function more frequently than vital teeth. This observation has been attributed to compromised clinical crown structure and to an unsubstantiated notion that non-vital dentin is more brittle than vital dentin. Huang, Schilder and Nathanson (1992) found non-vital dentin to be as strong and tough as vital dentin. I propose that non-vital teeth lack intradental proprioception and often fracture due to excessive functional occlusal forces generated by minimally restrained masticatory muscles. Loewenstein and Rathkamp (1955) observed an average increase of 57% in the threshold of pressure perception of non-vital teeth compared to vital teeth using axially applied forces. They also observed an average increase of 127% in the threshold of pressure perception of crowned vital teeth compared to intact vital teeth. Randow and Glantz (1986) found that "non-vital teeth had mean pain threshold levels that, on cantilever loading, were more than twice as high as those of neighboring or contralateral vital teeth.". Their study was discontinued for ethical reasons when a non-vital tooth fracture in dentin occurred during experimental loading. The oral musculature is capable of generating maximum bite forces much greater than the forces required to fracture teeth.

I propose that cyclic occlusal forces generate significant compressive stresses which induce material fatigue fractures in dentin that propagate along planes of maximum shear stress. Compressive/shear fatigue fractures will propagate in an ideal material at a 45 degree angle (Fig. 7). "V" shaped cervical abfractions are the clinical manifestations of accumulated compressive/shear fatigue damage in teeth which are subjected to excessive occlusal forces. The variation in abfraction plane angles encountered in clinical situations is dependent on elemental stresses which are resultants of of tooth contact force vectors, tooth geometry and material properties. The location of future abfractions on a tooth can be predicted by calculating the distribution of axial, bending, torsional and shear stresses and determining the position of elements which are most highly stressed. In time, as peripheral cervical elements of dentin fail and chip away, the cross-sectional area of the tooth is reduced. This produces a decrease in the area moment of inertia of the section, an increase in stress and a pronounced decrease in the load carrying capacity of the tooth. The lateral loading with 50% abfraction analysis illustrates the effect a reduced area moment of inertia has of significantly reducing the load carrying capacity of a tooth. Additional overloading of cervical dentin produces continuous material failure and enlargement of the abfraction.

According to Jastrzebski (1976) a common characteristic of all material fatigue fractures is a region of smooth, highly polished material which is the origin of the fatigue failure. Fatigue failure in composite materials often begins with interface debonding which leads to microcracks. I propose that abfractions often form at the cervical terminus of the DEJ. This region is highly stressed as a result of occlusal force generated bending, axial and torsional stresses and undergoes interface debonding of enamel and dentin after a sufficient number of stress cycles have occurred. The smooth dentin surfaces characteristic of most abfractions are an indication that a fatigue failure is in progress. The variation in abfraction morphology can be attributed to the stage of development of a compressive/shear or tensile fatigue failure of dentin and enamel. Compressive/shear abfractions are likely to be angular "V" shaped lesions and tensile abfractions are likely to be saucer shaped. Further structural analysis, material testing and clinical correlation is required for a more definitive morphologic understanding of abfractions.

Gay *et al.* (1994) found functional bite force magnitudes to be correlated with the physical properties of the food bolus incised but not to the strength of an individuals oral musculature. The proprioceptive neuromusculature limited bite forces to the levels required to achieve bolus fracture regardless of an individuals maximum bite force capability. The long term survival of teeth severely weakened by abfractions demonstrates the role of intradental proprioceptors. Intradental proprioception, in concert with neuromuscular masticatory reflexes, protects weakened teeth from immediate occlusal overload and fracture during mastication. Abfractions are an indication that existing masticatory chewing patterns have created a condition of excessive occlusal loading. The proprioceptive neuromusculature is capable of restraining occlusal loading from inducing excessive strains in vital dentin which will cause immediate fracture. The proprioceptive neuromusculature does not appear capable of restraining occlusal loading from causing accumulated fatigue damage in vital dentin which will ultimately result in fatigue failure. It is unlikely that periodontal proprioceptors alone are capable of monitoring occlusal forces adequately to prevent occlusal overload and fracture of teeth severely weakened by abfractions. Due to their external location, periodontal proprioceptors can only sense tooth movements. These movements include tooth translations and rotations and possibly root bending. The perception of complex strains in dentin is limited to intradental proprioceptors.

I postulate that intradental proprioceptors are located in the plethora of odontoblastic tubules which permeate dentin. I propose the term "odontoblastic sensory unit " (OSU) to describe the odontoblastic tubule, the odontoblastic process and associated nerve fiber, and the peri-odontoblastic fluid (Fig. 1 and Fig. 2). Loewenstein (1971) proposed the transducer mechanism of the Pacinian corpuscle. Compression of the relatively elastic surface membrane of the dendrite ending in the Pacinian corpuscle reduces the membrane resistance to ion flow. Charge is then transferred across the membrane by ions moving along their electochemical gradients. This

generator current produces an action potential. Theories as to the etiology of the impulses responsible for tooth pain have been developed. These include the direct enervation theory, the odontoblastic transduction theory and the hydrodynamic theory (Dubner *et al.*, 1978) . It is possible that aspects of each theory may participate in the mechanism of intradental proprioception.

Following is my theory describing the transducer mechanism of the OSU. The calcium ion concentration of intertubular dentinal fluid normally should be lower than that of periodontoblastic fluid due to a concentration gradient established by OPs and the high degree of calcification of peritubular dentin. Hypocalcemia has been shown to increase axonal excitability. Occlusal forces cause compression of intertubular dentin which induces flow of hypocalcemic intertubular dentinal fluid through canaliculi into OTs toward the pulp chamber. The osmotic membrane resting potential of nerve fibers in OTs is altered by the flow and pressure of this hypocalcemic fluid and action potentials (APs) are generated. Compression of the membrane may reduce membrane resistance to ion flow as Lowenstein theorized in the Pacinian corpuscle. Haljamäe and Röckert (1970) demonstrated that the OP contains a high level of intracellular potassium which may diffuse into the peri-odontoblastic fluid. This would further increase the excitability of afferent nerve fibers in the OSU (Scott, 1977). Control of osmotic equilibrium may be facilitated by OP potassium levels. Hirata *et al.* (1991) observed significant hydrodynamic fluid flow from dentinal tubules which were compressed by axially applied forces. They correlated the loading of dentin with APs recorded in the inferior alveolar nerve. APs have been shown to be generated by nerve fibers in dentin as a result of exposure to altered osmotic pressure (Orchardson, 1977; Horiuchi and Matthews, 1974). I propose that OSUs monitor occlusal forces and function as proprioceptors by reacting to changes in osmotic and fluid pressures initiated by tooth contacts. Further microanalytic research is needed for verification and enhancement of this theory.

APs generated in OSU proprioceptors travel along pulpal nerve fibers and stimulate neuromuscular masticatory reflexes. Masticatory reflexes regulate the magnitude of occlusal forces and resulting tooth deformations. This continuous feedback loop is augmented by periodontal and musculoskeletal proprioceptors. It operates as a self limiting protective mechanism. The variation in published maximum bite force values is in part a direct result of this regulatory mechanism. Based on their experiments with human subjects Mao and Osborn (1994) concluded that "the direction of of a bite force, not its magnitude determines the pattern of activity of jaw closing muscles." It is likely that most experimentally derived maximum bite force values were obtained under axial loading conditions which in producing minimum stress are an indication of the maximum load carrying capacity of an inividuals teeth. These values also reflect the proprioceptive sensitivity of an individuals teeth. The variables which must be included in an equation describing maximum bite force include force magnitude and direction, tooth material properties, restorative material properties, degree of tooth vitality, periodontal support, and the strength of the

surrounding musculoskeletal system including the TMJs. These variables influence tooth flexure and the sensitivity of the proprioceptive system. OSUs, which uniquely occupy regions of high intradental stress, limit biting forces below maximum material strain deformation values of dentin.

The failures observed clinically in teeth (including abfractions) are usually generated under cyclic loading conditions which induce material failures at sub-strength values. This phenomenon explains the occurrence of the cuspal fracture for which the patient attributes the cause to be biting on soft food. Progressive failure of teeth and subsequent restoration impairs intradental proprioceptive function and subjects all components of the masticatory system to increasing occlusal force magnitudes. The result is accelerated destruction of masticatory system components.

Early analysis of occlusions and occlusal therapeutic methods such as those advocated by Dawson (1989) are imperative for the long term maintenance of the masticatory system. These methods distribute masticatory forces maximally, eliminate destructive lateral force-induced bending stresses and minimize reflex muscular activity initiated by proprioceptor stimulation. Failure to adhere to these principles may be responsible for creating the delta stage bruxer. In this case, reduced intradental proprioception is the result of bruxism, occlusal wear, scleroic dentin formation, fractured teeth, non-vital teeth, extracted teeth and extensive prosthetic reconstruction. The delta stage bruxer exhibits an overdeveloped musculature with a severely diminished proprioceptive capacity. The result is a masticatory system which self destructs.

Consideration of the biomechanical and neurophysiological concepts outlined in this article is intended to aid clinicians in the preservation of masticatory system structure and function. Clinical research and theoretical studies advancing these concepts are strongly encouraged.

APPENDIX

This appendix contains computational procedures used in the structural analysis.

Axial loading

Section A maximum normal stress:

F = -25 lb (-111 N), A = 0.0390 in.^{2} (25.2 mm^2).

(eq-1) $\sigma_A = F/A$ = -640 lb/in.^{2} (-4.4 MPa): uniform compression across section.

Section B maximum normal stress:

F = -25 lb (-111 N), A = 0.0262 in.^{2} (16.9 mm^2).

(eq-1) $\sigma_A = F/A$ = -950 lb/in.^{2} (-6.6 MPa): uniform compression across section.

A reduction of cross sectional area due to the conical root form of a maxillary central incisor with crestal bone loss produces an increase in axial normal stress at critical sections.

Inclined loading

The 25 lb (111 N) force may be expressed as x, y and z components:

$F_x = F_y$ = -25 (sin 45°) = -17.7 lb (-79 N), $F_z = 0$ (F intersects the neutral axis).

Section A maximum normal stresses (at element: A_1):

(eq-1) $\sigma_A = F_y / A$: F_y = -17.7 lb (-79 N), A = 0.0390 in.^{2} (25.2mm^2).

σ_A= -450 lb/in.^{2} (-3.1 MPa): uniform compression over entire section.

(eq-2) $\sigma_B = \frac{Mc}{I}$: $M = F_x(L) - F_y(e) = -17.7(0.335) + 17.7(0.039)$

M = -5.24 in.•lb (-592 N•mm)

$c_{max} = r_o$ = 0.114 in. (2.9 mm)

$I = (\pi/4)(r_o^4 - r_i^4) = (\pi/4)(1.69(10^{-4}) - 3.32(10^{-7}))$

I = 1.32(10^{-4}) in.^{4} (54.9 mm^4)

σ_{Bmax}= -4,530 lb/in.^{2} (-31.2 MPa): compression.

σ_{A+Bmax} = -450 lb/in.^{2} – 4,530 lb/in.^{2} = -4,980 lb/in.^{2} (-34.3MPa): compression.

Equation 2 (the flexure formula) predicts that the bending stress at a section varies from zero along the neutral axis of the section to σ_{Bmax}. This maximum bending stress occurs at elements which are the maximum distance from the neutral axis of the section ($c_{max} = r_o$). Therefore, under this loading condition the extreme buccal and extreme lingual points of the section, elements A_1 and A_5 respectively, are subjected to the greatest normal stresses: A_1 compression and A_5 tension. This equation also shows that bending stress is directly proportional to the applied bending moment. Increasing F_x and L. have the effect of increasing M by direct proportion. The eccentric moment arm, e, has the effect of creating a counter moment to the moment induced by the horizontal force component (F_x). The radius of a section has a pronounced effect on the I of the section. A decrease in section radius causes an exponential fourth power decrease in I and a dramatic increase in bending stress. This effect is restrained by one exponential power of radius due to the c variable. As the I data reflects, the presence of the pulp has only a small effect on the area moment of inertia and thus only minimally effects bending stress.

Section A maximum shear stresses (at element A_3):

(eq-3) $\tau_L = \frac{VQ}{It}$: $V = F_x$ = -17.7 lb (-79N)

$Q_{max} = (\bar{a}_x)(A/2)$ = 9.8(10^{-4}) in.^{3} (16.1 mm^3)

$\bar{a}_x$ = 0.050 in. (1.3 mm): 1/2 section centroid to neutral axis.

I = 1.32(10^{-4}) in.^{4} (54.9 mm^4)

$t_{max} = 2(r_o - r_i)$ = 0.180 in. (4.6mm)

τ_{Lmax} = +730 lb/in.^{2} (+5.0 MPa): positive shear.

The shear stress due to lateral force is greatest along the neutral axis of a section of a tooth. This finding relates to the maximum value of Q. $\tau_L = 0$ at a distance of r_o from the neutral axis or at elements A_1 and A_5. Increasing the pulp radius increases τ_L by decreasing t. As in bending stress, decreasing the radius of a section has a marked effect on I and increases τ_L accordingly. τ_L is also directly proportional to V (the lateral force component equal to F_x). The numerical results

obtained in applying (eq-3) to dentin, a non-homogeneous orthotropic material, must be considered approximate.

(eq-4) $\tau_T = \frac{Ty}{J}$ $\tau_T = 0$ lb/in^2

No torque is applied to the model tooth due to the intersection of the applied force vector with the neutral axis of the tooth. Centralized placement of occlusal forces will eliminate the torsional component of shear stress. According to this equation, in the presence of an applied torque, shear stress increases linearly from zero at the center of a tooth section to a maximum at the perimeter of the section ($y = r_o$). A larger cross-sectional area will increase the polar moment of inertia of that area (J) and decrease shearing stress due to torsion. In this example τ_T is also maximum when coincident with the two elements of greatest bending stress (A_5 tension and A_1 compression) and at two elements of greatest shear stress (positive shear at both the mesial and distal peripheral elements of the neutral axis of the section).

Section B maximum normal stresses (at element B_1):

(eq-1) $\sigma_A = F_y / A$: F_y = -17.7 lb (-79N), A = 0.0262 in.^{2} (16.9 mm^2).

σ_A = -680 lb/in^2 (-4.7 MPa): compression over entire section.

(eq-2) $\sigma_B = \frac{Mc}{I}$: $M = F_x(L') - F_y(e)$ = -17.7(0.488)+17.7(0.039)

M = -7.95 in.•lb (-898 N•mm)

$c_{max} = r_o$ = 0.094 in. (2.4 mm)

$I = (\pi/4)(r_o^4 - r_i^4) = (\pi/4)(7.81(10^{-5}) - 2.34(10^{-7}))$

$I = 6.12(10^{-5})$in.^{4} (25.5 mm^4)

σ_{Bmax} = -12,200 lb/in.^{2} (-84.1 MPa): compression.

σ_{A+Bmax} = -680 lb/in.^{2} -12,200 lb/in.^{2} = -12,880 lb/in.^{2} (-88.8 MPa): compression.

Table 1. Mechanical properties.*

	Dentin		Enamel	
	lb/in.^{2}	MPa	lb/in.^{2}	MPa
Elastic Modulus, *E*	2.65 (10^6)	18,300	12.2 (10^6)	84,100
Tensile Strength, UTS	(6.0-7.5)(10^3)	41.4-51.7	1.5 (10^3)	10.3
Shear Strength, G	(14.8-20.0)(10^3)	102-138	13.1 (10^3)	90.2
Proportional Limit, PL	24.2 (10^3)	167	51.2 (10^3)	353
Compressive Strength, C	43.1(10^3)	297	55.7 (10^3)	384

*From O'Brien (1989). PL tested in compression.

Table 2. Stress levels in the maxillary central incisor tooth model loaded with a 25 lb (111 N) axial force.

Section A:	0% Bone Loss									
	Element A_1		Element A_2		Element A_3		Element A_4		Element A_5	
	lb/in^2	MPa	lb/in^2	MPa	lb/in^2	MPa	lb/in^2	MPa	lb/in^2	MPa
Normal Stress	-640	-4.4	-640	-4.4	-640	-4.4	-640	-4.4	-640	-4.4
Shear Stress	0	0	0	0	0	0	0	0	0	0
Section B:	30% Bone Loss									
	Element B_1		Element B_2		Element B_3		Element B_4		Element B_5	
	lb/in^2	MPa	lb/in^2	MPa	lb/in^2	MPa	lb/in^2	MPa	lb/in^2	MPa
Normal Stress	-950	-6.6	-950	-6.6	-950	-6.6	-950	-6.6	-950	-6.6
Shear Stress	0	0	0	0	0	0	0	0	0	0

Table 3. Stress levels in the maxillary cental incisor tooth model loaded with a 25 lb (111 N) force inclined at 45 degree.

Section A:	0% Bone Loss									
	Element A_1		Element A_2		Element A_3		Element A_4		Element A_5	
	lb/in^2	MPa	lb/in^2	MPa	lb/in^2	MPa	lb/in^2	MPa	lb/in^2	MPa
Axial Stress	-450	-3.1	-450	-3.1	-450	-3.1	-450	-3.1	-450	-3.1
Bending Stress	-4530	-31.2	-950	-6.6	0	0	+950	+6.6	+4530	-31.2
Normal Stress	-4980	-34.3	-1400	-9.7	-450	-3.1	+500	+3.5	+4080	-28.1
Shear Stress	0	0	+550	+3.8	+730	+5.0	+550	+3.8	0	0
Section B:	30% Bone Loss									
	Element B_1		Element B_2		Element B_3		Element B_4		Element B_5	
	lb/in^2	MPa	lb/in^2	MPa	lb/in^2	MPa	lb/in^2	MPa	lb/in^2	MPa
Axial Stress	-680	-4.7	-680	-4.7	-680	-4.7	-680	-4.7	-680	-4.7
Bending Stress	-12200	-84.1	- 2860	-19.7	0	0	+2860	+19.7	+12200	+84.1
Normal Stress	-12880	-88.8	-3540	-24.4	-680	-4.7	+2180	+15.0	+11520	+79.5
Shear Stress	0	0	+810	+5.6	+1130	+7.8	+810	+5.6	0	0

Normal stress from axial force:

$$\sigma_A = F/A \qquad (1)$$

Normal bending stress from lateral force:

$$\sigma_B = \frac{Mc}{I} \qquad (2)$$

Shear stress from lateral force:

$$\tau_L = \frac{VQ}{It} \qquad (3)$$

Shear torsional stress from eccentric force application:

$$\tau_T = \frac{Ty}{J} \qquad (4)$$

Variables

F : applied force. In model $F = 25$lb (111 N).

A : cross sectional area. In model: $A=\pi(r_o^2 - r_i^2)$, where r_o is the outer section radius and r_i is the inner section radius.

M : bending moment. In model, $M = F_x(L) - Fy(e)$, where F_x and Fy are the x and y components of F, L is the lateral force moment arm, e is the eccentric moment arm.

c : distance of the considered element from neutral axis.

I : area moment of inertia of the section. In model, $I = (\pi/4)(r_o^4 - r_i^4)$.

V : shear force applied.

Q : first or statical moment of an area about the neutral axis.

t : width of longitudinal cut considered.

T : applied torque.

J : polar moment of inertia of the section. In model, $J = I / 2$.

REFERENCES

Arsenault, A. and Robinson, B. (1989) The dentino-enamel junction: a structural and microanalytical study of early mineralization. *Calcified Tissue International* **45**, 111-121.

Arwill, T., Edwall, L., Lilja, J., Olgart, L. and Svensson, S-E. (1973) Ultrastructure of nerves in the dentinal-pulp border zone after sensory and autonomic nerve transection in the cat. *Acta Odontal Scand* **31**, 273-281.

Avery, J. K. (1992) *Essentials of Oral Histology and Embryology: A Clinical Approach*, pp.93-104. Mosby-Year Book Inc., St. Louis.

Bjornland, T., Brodin, P. and Aars, H. (1991) Force-related changes in the masseter muscle reflex response to tooth-taps in man. *J. of Oral Rehabilitation* **18**, 125-132.

Braden, M. (1976) *Frontiers of Oral Physiology, Vol. 2: Physiology of Oral Tssues*, p.15. S.Karger AG, Basel.

Byers, M. R. and Kish, S. J. (1976) Delineation of somatic nerve endings in rat teeth by radioautography of axon-transported protein. *J. Dent. Res.* **55**, No. 3, 419-425.

Caputo, A. A. and Standlee, J. P. (1987) *Biomechanics in Clinical Dentistry.* Quintessence, Chicago.

Darendeliler, S., Darendeliler, H. and Kinoglu, T. (1992) Analysis of a maxillary incisor by using a three-dimensional finite element method. *J Oral Rehabilitation* **19**, 371-383.

Dawson, P. E. (1989) *Evaluation, Diagnosis and Treatment of Occlusal Problems* (2nd Edn), Mosby, St Louis.

Dong, W. K., Chudler, E. H. and Martin, R.F. (1985) Physiological properties of intradental mechanoreceptors. *Brain Research* **334**, 389-395.

Dong, W. K., Shiwaku, T., Kawakami, Y. and Chudler, E. H. (1993) Static and dynamic responses of periodontal ligament mechanoreceptors and intradental mechanoreceptors. *Journal of Neurophysiology* **69**, No. 5, 1567-1582.

Dubner, R., Sessle, B. J. and Storey, A. T. (1978) *The Neural Basis of Oral and Facial Function*, pp. 118-130. Plenum Press, New York.

Farah, J. W., Craig, R. G. and Sikarskies, D. L. (1973) Photoelastic and finite element stress analysis of a restored axisymetric first molar. *J. Biomechanics* **6**, 511-520.

Frank, R. M. (1968) Attachment sites between the odontoblast process and the intradentinal nerve fiber. *Archs oral Biol.* **13**, 833-834.

Fosse, G., Saele, P. K. and Eide, R. (1992) Numerical density and distributional pattern of dentin tubules. *ACTA Odontol Scand* . **50**, 201-210.

Gay, T., Rendell, J., Majoureau, A. and Maloney, F. T. (1994) Estimating human incisal bite forces from the electromyogram/bite-force function. *Archs oral Biol.* **39**, 111-115.

Garberoglio, R. and Brannstrom, M. (1976) Scanning electron microscopic investigation of human dentinal tubules. *Archs oral Biol* . **21**, 355-362.

Goel, V. K., Khera ,S. C. and Sing, K. (1990) Clinical implications of the response of enamel and dentin to masticatory loads. *J Prosthet Dent* . **64**, 446-454.

Grippo, J. O. (1991) Abfractions: a new classification of hard tissue lesions of teeth. *Journal of Esthetic Dentistry* . **3**, No. 1, 14-19.

Gurza, S., Lowe, A. A. and Sessle, B. J. (1976) Influences on masseter muscle activity of stimuli applied to various sites in cats and macaque monkeys. *Archs. Oral Biol.* **21**, 705-707.

Haljamäe, H. and Röckert, H. (1970) Potassium and sodium content in dentinal fluid. *Odontologisk Revy.* **21**, 369-377.

Hirata, K., Nakashima, M., Sekine, I., Mukouyama, Y. and Kimura, K. (1991) Dentinal fluid movement associated with loading of restorations. *J Dent. Res.* **70**(6), 975-978.

Hoijatie, B. and Anusavice, K. J. (1990) Three dimensional finite element analysis of glass-ceramic dental crowns. *J. Biomechanics.* **23**(11), 1157-1166.

Horiuchi, H. and Matthews, B. (1974) Evidence on the origin of nerve impulses recorded from dentine in the cat. *J. Physiol. (London)* **243**, 797-829.

Holland, G. R. (1976) Lanthanum hydroxide labeling of gap junctions in the odontoblast layer. *Anat Rec.* **186**, 121-126.

Huang, T-J. G., Schilder, H. and Nathanson, D. (1992) Effects of moisture content and endodontic treatment on some mechanical properties of human dentin. *J. Endodontics* **18**(5), 209-215.

Jastrzebski, Z. D. (1976) *The Nature and Properties of Engineering Materials* (2nd Edn), pp. 274-277. Wiley, New York.

Kawamura, Y. (1976) *Frontiers of Oral Physiology, Vol. 2: Physiology of Oral Tissues,* p.15. S. Karger, Basel.

Kodaka, T., Hirayama, A., Abe, M. and Miake K. (1992) Organic structures of the hypercalcified peritubular matrix in horse dentin. *Acta Anat* . **145**, 181-188.

Kraus, B. S., Jordan, R. E. and Abrams, L. (1969) *Dental Anatomy and Occlusion.* Williams and Wilkins, Baltimore.

Lavelle, C. L. B. (1988) *Applied Oral Physiology,* p. 16. Butterworths, London.

Lee, W. C., Eakle, W. S. (1984) Possible role of tensile stress in the etiology of cervical erosive lesions of teeth. *J. Prosthet. Dent.* **52**, No. 3, 374-380.

Lowenstein, W. R. (1971) *Principles of Receptor Physiology,* pp. 269-290. Springer-Verlag, New York.

Lowenstein, W. R. and Rathkamp, R. (1955) A study on the pressoreceptive sensibility of the tooth. *J. Dent. Res.* **34**, 287-294.

Mao, J., Osborn, J. W. (1994) Direction of a bite force determines the pattern of activity in jaw closing muscles. *J. Dent Res.* **73**, No. 5, 1112-1120.

Marion, D., Jean, A., Hamel, H., Kerebel, L-M and Kerebel, B. (1991) Scanning electron microscopic study of odontoblasts and circumpulpal dentin in a human tooth. *Oral Surg Oral Med Oral Pathol.* **72**, 473-478.

Matthews, B. (1981) Human and animal studies on receptor mechanisms in teeth. *Oral-Facial Sensory and Motor Functions* (Edited by Kawamura, Y. and Dubner, R.), pp. 269-271. Quintessence, Tokyo.

McGrath, P.A., Sharav, Y., Dubner, R. and Gracely, R.H. (1981) Masseter inhibitory periods and sensations evoked by electrical tooth pulp stimulation. *Pain*. **10**, 1-17.

O'Brien, W. J. (1989) *Dental Materials: Properties and Selection.* Quintessence, Chicago.

Olgart, L., Gazelius, B. and Sundström, F. (1988) Intradental nerve activity and jaw opening reflex in response to mechanical deformation of cat teeth. *Acta Physiol Scand.* **133**, 399-406.

Orchardson, R. (1977) Ion sensitivity of intradental nerves in the cat. *Pain In the Trigeminal Region* (Edited by Anderson, D. J. and Matthews B), pp. 77-82. Elsevier/North-Holland Biomedical Press, Amsterdam.

Phillips, R. W. (1973) *Skinner's Science of Dental Materials* (7th Edn), pp. 49-51. Saunders, Philadelphia.

Popov, E. P. (1976) *Mechanics of Materials* (2nd Edn). Prentice-Hall, New Jersey.

Randow, K., Glantz, P. (1986) On cantilevered loading of vital and non-vital teeth. *Acta Odontol Scand* **44**, 271-277.

Scott, D. (1977) Intradental receptor duality. *Pain in the Trigeminal Region* (Edited by Anderson, D. J. and Matthews, B.), pp. 67-76. Elsevier/North-Holland Biomedical Press, Amsterdam.

Selna, L. G., Shillingberg, H. T. Jr. and Kerr, P. A. (1975) Finite element analysis of dental structures-axismetric and plane stress idealizations. *J. Biomed. Mater. Res.* **9**, 237-252.

Sogaard-Pedersen, B., Boye, H. and Matthiessen, E. (1990) Scanning electron microscope observations on collagen fibers in human dentin and pulp. *Scand J. Dent Res.* **98**, 89-95.

Szabo, J., Trombitas, K. and Szabo, I. (1984) The odontoblast process and its branches in human teeth observed by scanning electron microscopy. *Arch. Oral Biol.* **29**(4), 331-333.

Taylor, A. (1990) *Neurophysiology of the Jaws and Teeth*, pp. 57-69. Macmillan, London.

Thresher, R. W. and Saito, G. E. (1973) The stress analysis of human teeth. *J. Biomechanics.* **6**, 443-449.

Yettram, A. L., Wright, K. W. J. and Pickard, H. M. (1976) Finite element stress analysis of the crowns of normal and restored teeth. *J. Dent. Res.* **55**(6), 1004-1011.

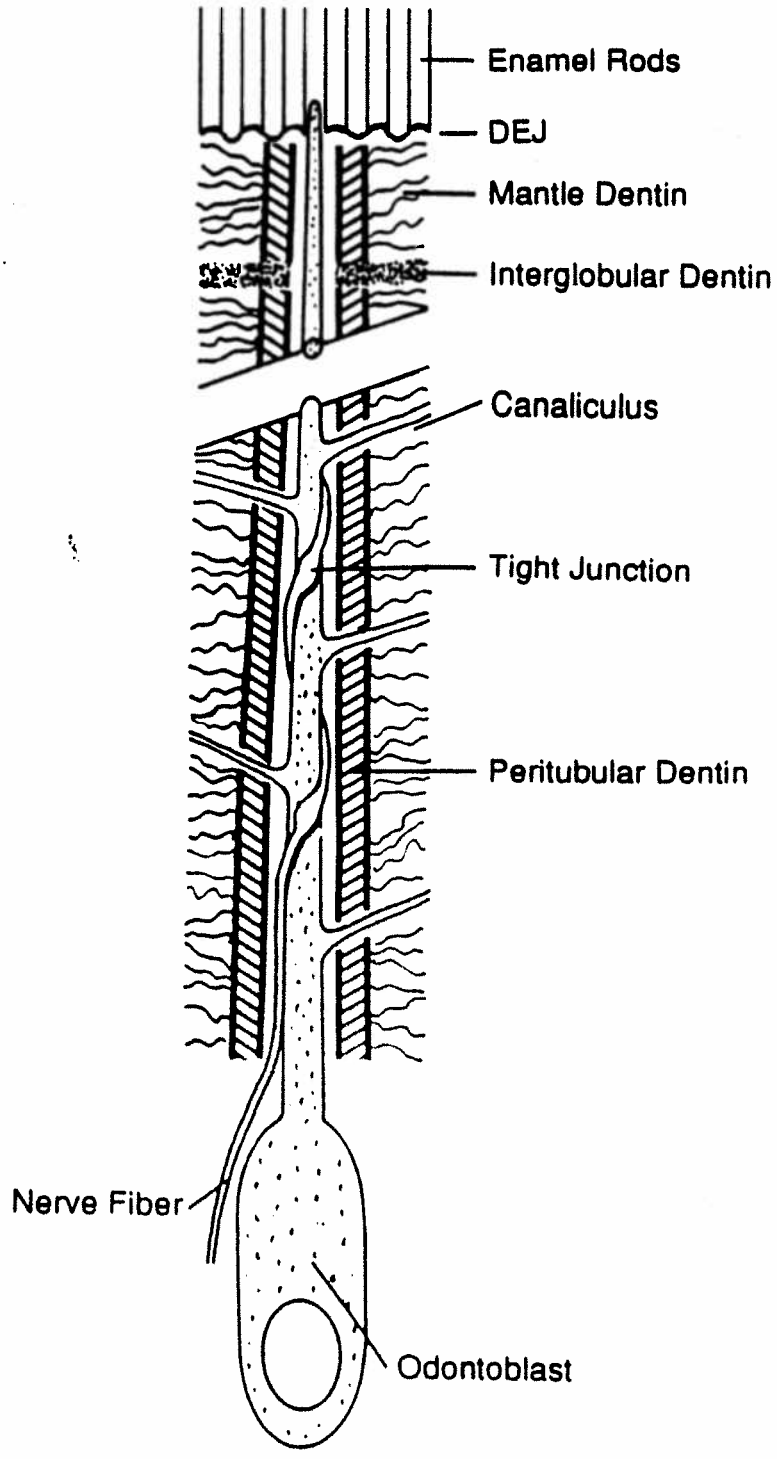
Enamel Rods
DEJ
Mantle Dentin
Interglobular Dentin
Canaliculus
Tight Junction
Peritubular Dentin
Nerve Fiber
Odontoblast

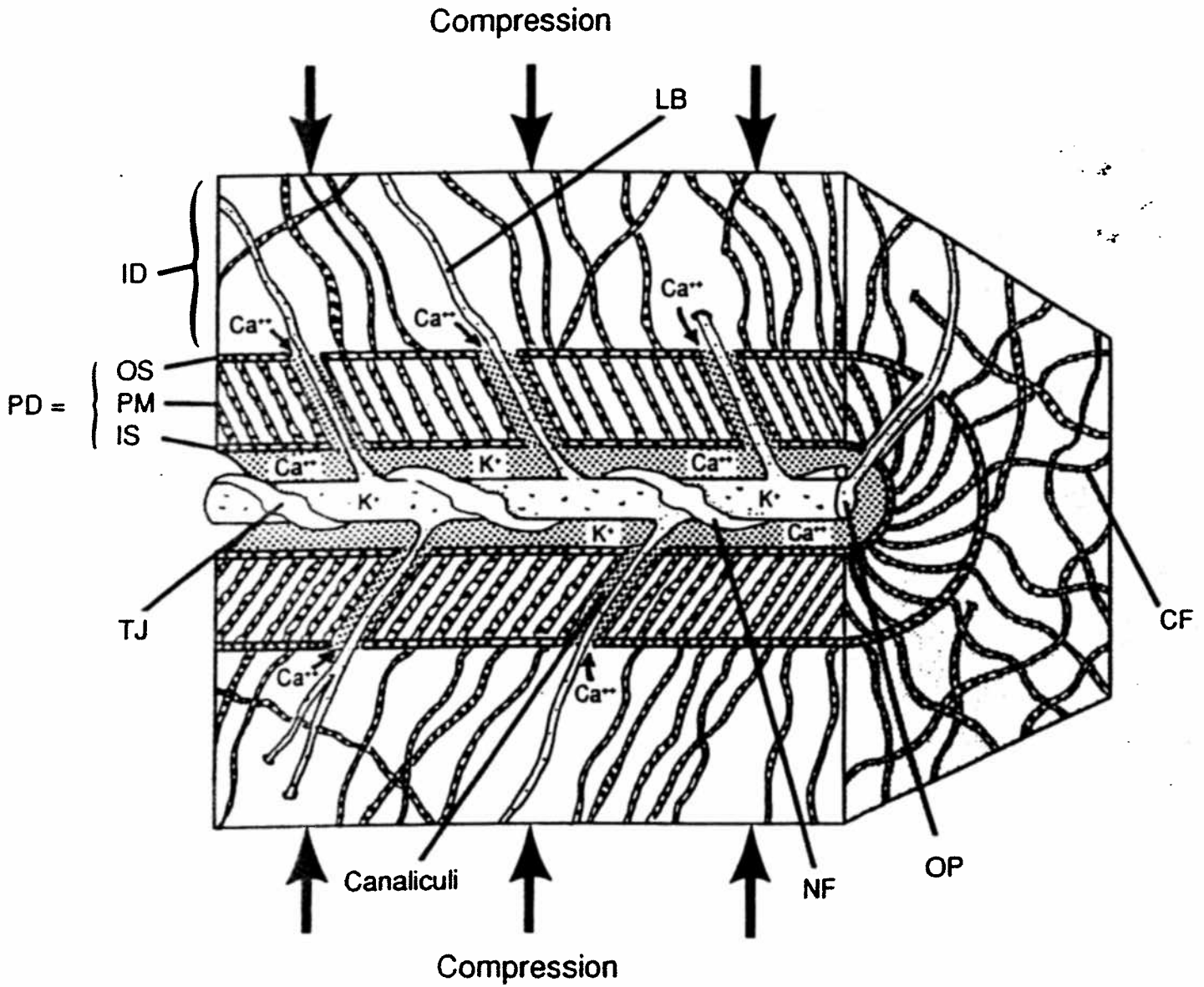
Compression
LB
ID
PD =
OS
PM
IS
Ca++
K+
TJ
CF
Canaliculi
NF
OP
Compression

Maxillary Right Central Incisor

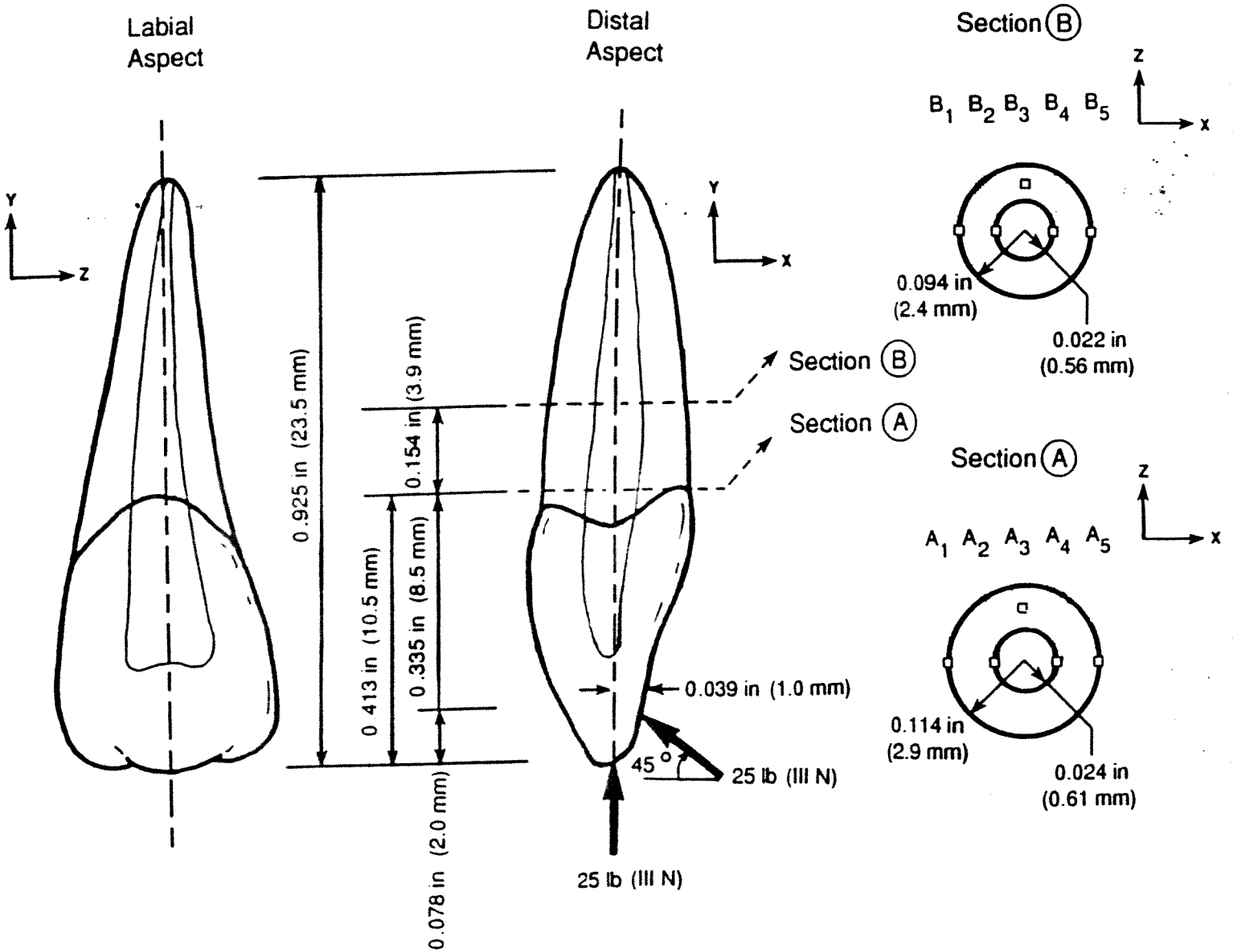

Section A

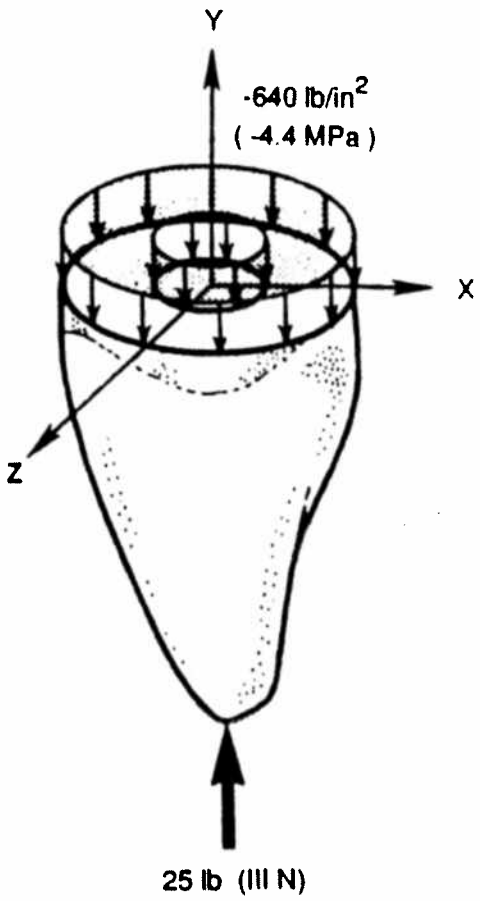

Section B

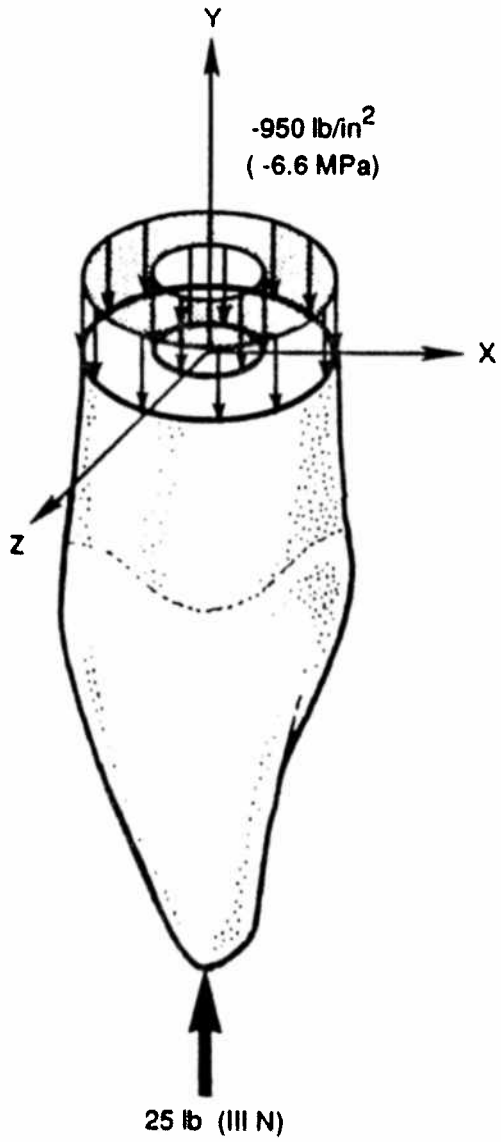

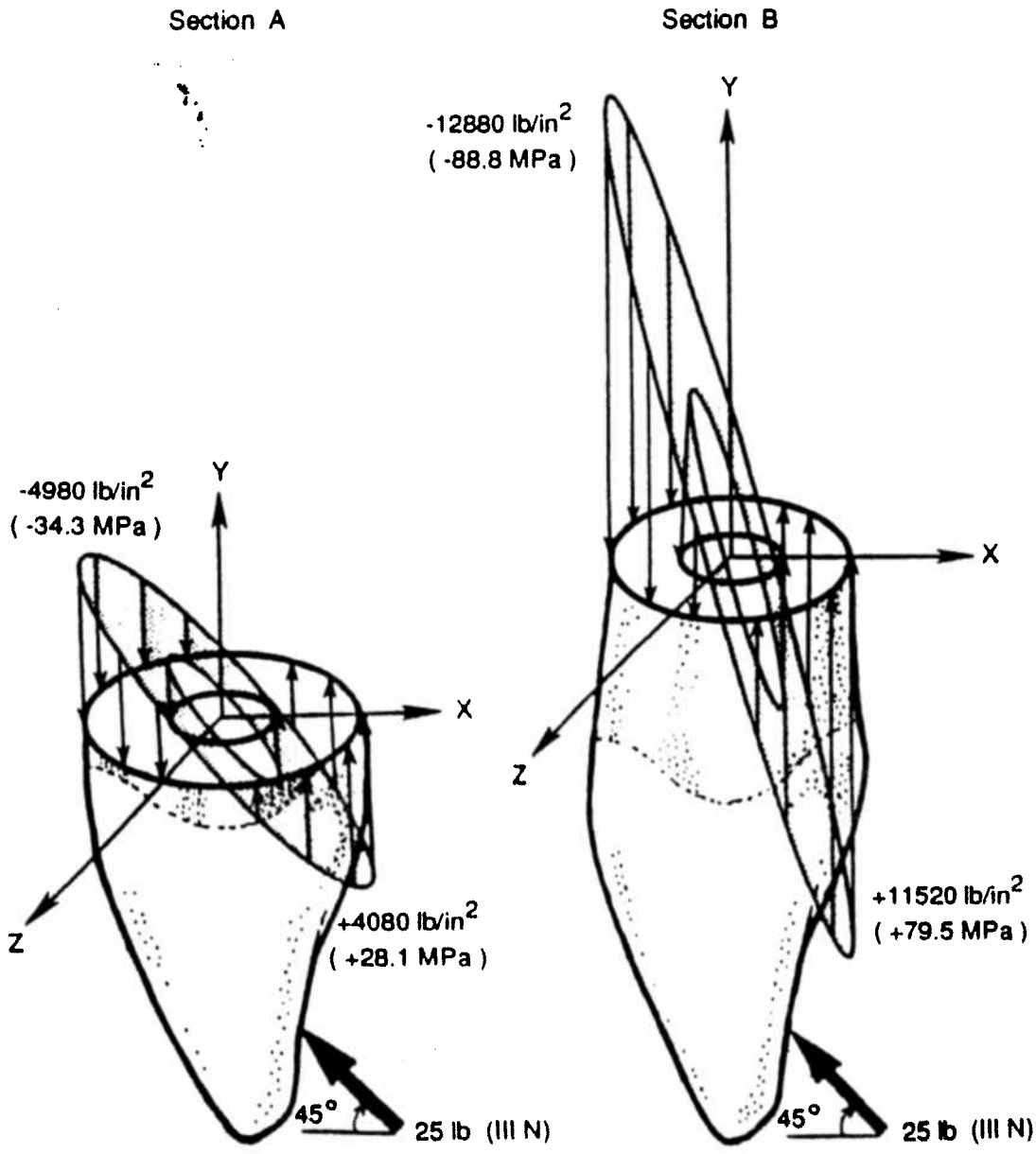
Section A
Section B
-12880 lb/in2
(-88.8 MPa)
Y
X
Z
-4980 lb/in2
(-34.3 MPa)
+4080 lb/in2
(+28.1 MPa)
45°
25 lb (III N)
+11520 lb/in2
(+79.5 MPa)
45°
25 lb (III N)

Equivalent Stress States

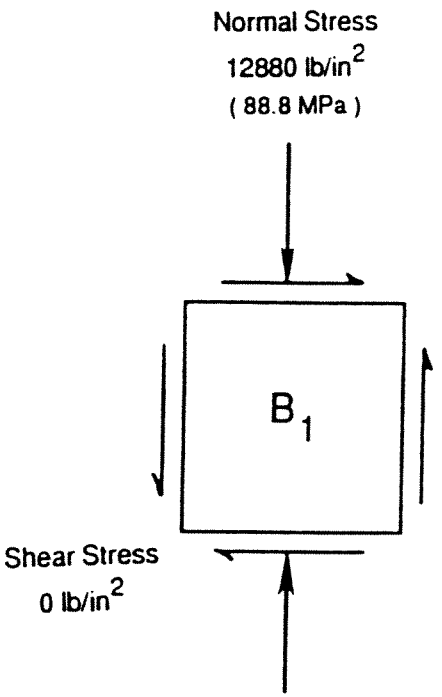

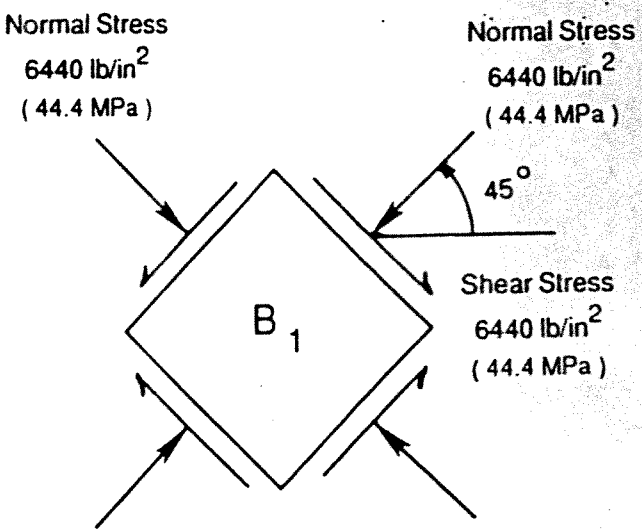

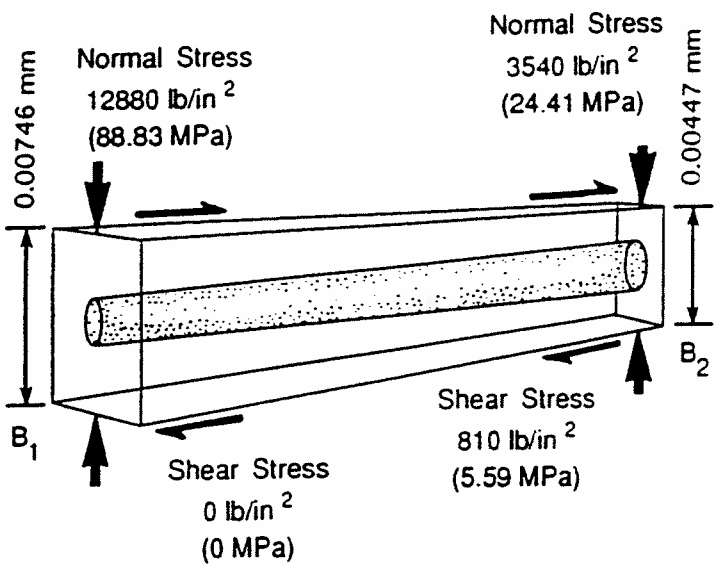

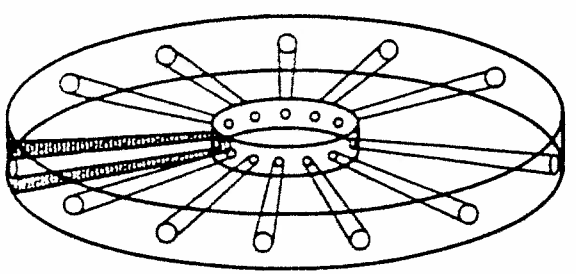

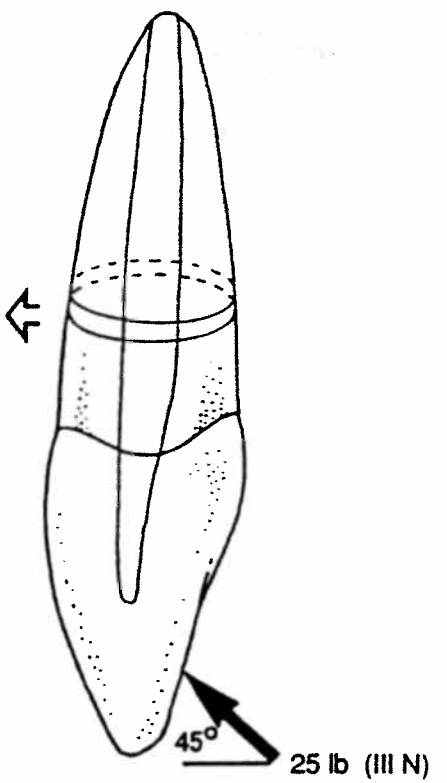

Ratio of Deformation

$B_1 : B_2$

6.05 : 1.00

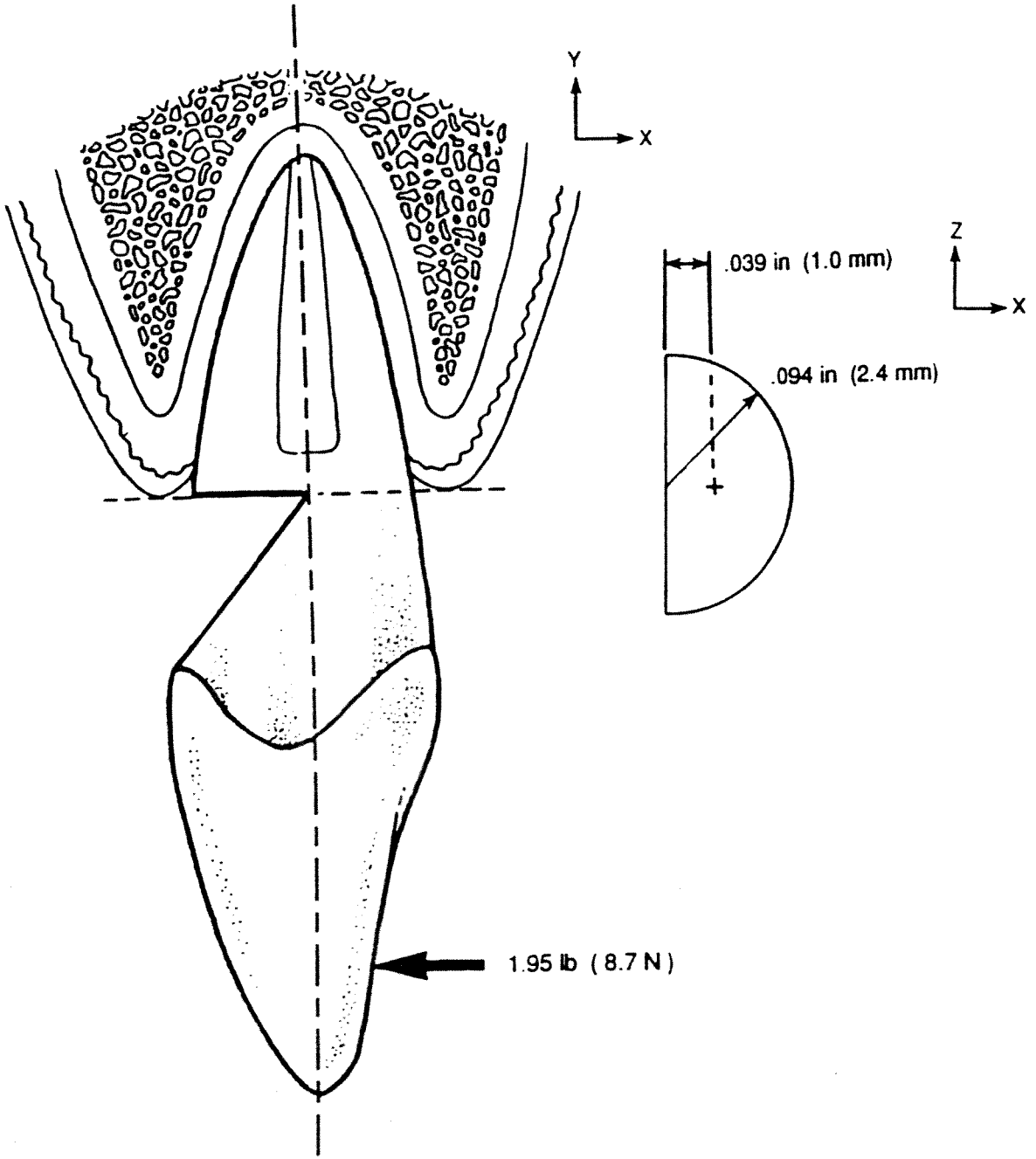
Y
X
Z
X
.039 in (1.0 mm)
.094 in (2.4 mm)
1.95 lb (8.7 N)

Fig. 1. Schematic representation of an odontoblastic tubule (OT). I have named the functional unit this represents an odontoblastic sensory unit (OSU).

Fig. 2. Segment of odontoblastic sensory unit (OSU) in compression illustrating calcium ion flow into the odontoblastic tubule.* ID = Intertubular Dentin, PD = Peritubular Dentin, OS = Outer Fibrillar Sheath, PM = Peritubular Matrix, IS = Inner Sheath, OP = Odontoblastic Process, LB = Lateral Branch (of OP), NF = Nerve Fiber, TJ = Tight Junction.

*Adapted from: Kodaka, T., Hirayama, A., Abe, M. and Miake K. (1992) Organic structures of the hypercalcified peritubular matrix in horse dentin. *Acta Anat*. **145**, 181-188.

Fig. 3. Model of maxillary right central incisor. Section A represents normal periodontal bone support. Section B represents a 30% loss of supporting bone.*

*Adapted from: Kraus, B. S., Jordan, R. E. and Abrams, L. (1969) *Dental Anatomy and Occlusion*. Williams and Wilkins, Baltimore.

Fig. 4. Fundamental mechanical formulas.*

*Popov, E. P. (1976) *Mechanics of Materials*. (2nd Edn.) Prentice-Hall, New Jersey.

Fig. 5. Free body diagrams illustrating internal material normal stress distributions necessary to maintain equilibrium under axial loading conditions. The maxillary central incisor models are loaded with 25 lb (111 N) axial forces. Section A represents normal periodontal bone support. Section B represents a 30% loss of supporting bone.

Fig. 6. Free body diagrams illustrating internal material normal stress distributions necessary to maintain equilibrium under inclined loading conditions. The maxillary central incisor models are loaded with 25 lb (111 N) forces applied at 45 degree angles. Section A represents normal periodontal bone support. Section B represents a 30% loss of supporting bone.

Fig. 7. Stress transformation at element B_1 under inclined loading conditions showing the maximum shear stress as it occurs when element B_1 is rotated 45 degrees.

Fig. 8. Differential stress and deformation of an odontoblastic sensory unit (OSU) located in section B of under inclined loading conditions. The differential stress gradient between elements B_1 and B_2 results in the apical bending of the labial aspect of this OSU. The 6.05 : 1 ratio of deformation between elements B_1 : B_2 can be correlated to the volume of fluid which is displaced in an OSU due to the application of a 25 lb (111N) occlusal force applied at a 45 degree angle.

Fig. 9. Diagram of maxillary right central incisor with 30% bone loss and a 50% abfraction subjected to lateral loading conditions. The 1.95 lb (8.7 N) force indicated is the calculated maximum lateral load carrying capacity of thi severely weakened tooth.